

Novel Whole Brain DTI Segmentation and Diffusion Colour Mapping Technique for Tumour Diagnosis and Boundary Delineation

T. L. Jones¹, A. W. Chung², B. A. Bell¹, and T. R. Barrick²

¹Academic Neurosurgery Unit, St George's University of London, London, United Kingdom, ²Centre for Clinical Neurosciences, St George's University of London, London, United Kingdom

Introduction: Conventional MRI sequences (e.g. T1, T2 & FLAIR) have limited sensitivity and specificity in diagnosing brain tumours. Contrast enhanced image tumour boundaries may underestimate lesion margins, which is critical for image guided tumour resection and effective radiotherapy planning (given that maximal resection yields improved length of survival for both high and low grade glioma [1][2]). Previous studies have identified differences in diffusion patterns between tumour types [3] however this has yet to be applied in clinical practice. We present a novel whole brain DTI k-medians clustering algorithm that generate Diffusion Colour Maps (DCM). When this technique is applied to cases of intracranial mass lesions, the resultant DCMs display distinctive colour patterns for each tumour type with clearly delineated boundaries.

Methods: *MRI Data Acquisition:* Diffusion tensor MR scans were acquired from a normal subject and 7 patients (intracranial tumour selection (malignant (solid and cystic) & low grade glioma, metastasis, meningioma & lymphoma) and abscess). Subjects were scanned on a 1.5T General Electric Signa MRI. Diffusion-weighted images were acquired using a single shot spin-echo planar sequence (EPI) with 12 diffusion sensitised directions ($b=1000 \text{ s mm}^{-2}$), described previously [4]. In plane resolution was 2.5mm and through plane 2.8mm, providing near isotropic voxels. DTIs were computed as described previously [4] and isotropic (p) and anisotropic (q) metrics were calculated for each voxel [5].

Image Analysis - Initial Clustering: To ensure there was no bias in the clustering, each p and q map was rescaled to contain values between 0 and 1. Initial clustering involved the definition of 16 clusters. These were defined to express the range of tissue types present in brains with intracranial lesions (e.g. normal white matter, cortex, CSF spaces, tumour (solid component, necrotic core), tumour boundary, infiltrating edge and associated oedema, plus partial volume regions). The initial 16 clusters were defined in (p, q) space by the lower quartile, median and upper quartile values for p and q computed across the entire skull stripped brain image, I (Fig-1a). Clusters medians of p and q were then computed.

Image Analysis - K-Medians Clustering: Each image voxel, $i \in I$, was iteratively reclassified to one of the 16 clusters using k-medians clustering based on the distance in (p, q) space of the voxel (p_i, q_i) to its nearest cluster median (m_p, m_q) by,

$$\min_{j \in \{1, \dots, 16\}} \sqrt{(p_i - m_{pj})^2 + (q_i - m_{qj})^2}.$$

This was repeated for 100 iterations with a steady state of classification reached before termination. The final clustering of (p, q) space is shown in Fig-1b

Diffusion Colour Maps (DCM): Median p , q and T2 weighted intensities (T2 from the $b=0 \text{ s mm}^{-2}$ image) were computed for the final clusters. Median values were ranked according to magnitude to provide 3 grey-scale segmentations with values between 0 and 16 (Fig-1c). RGB colours were assigned to the grey-scale images by assigning the T2 cluster rank to the red channel, the p cluster rank to the green channel and the q cluster rank to the blue channel.

Results: Fig-2 displays DCMs and (p, q) space scatter plots following application of our algorithm (with corresponding conventional MRIs) for the range of intracranial pathology. The 'normal subject' displays characteristic DCM patterns; with blue representing white matter pathways (high q , low p), orange/purple representing cortex (low p and q) and pale yellow representing CSF spaces (high p , low q). Key findings include:

- Extent of tumour and oedema are larger than conventional MRI (e.g. T2 & FLAIR).
- Different colour patterns of oedema regions present (malignant glioma: light blue, metastasis; orange).
- Different colour patterns between abscess cavity and malignant glioma core (purple (for abscess), orange & olive green (for solid component of glioma core), and bright yellow (for tumour cystic component)).
- Different colour patterns of tumour core between malignant glioma and metastasis (heterogeneous orange & olive green vs. homogenous brown).
- Characteristic deep red of meningioma.

Discussion & Conclusions: The colour maps generated using our technique provides insight into cellular changes caused by these tumours. By incorporating T2 relaxation characteristics with diffusion patterns the DCM technique provides insight into micro-architectural differences between pathologies. The different oedema patterns observed in Fig-2 may be indicative of different pathologies, for example the infiltrative cellular oedema of glioma versus aqueous vasogenic oedema of metastases. As the discrimination of cystic malignant glioma and abscesses can be especially difficult in clinical practice our observed differences between the DCMs may reflect the viscous abscess core (i.e. restricted diffusion in all directions) and cystic necrosis of glioma (i.e. highly isotropic, aqueous). Variations in DCMs between tumour types represent differences in cell density and organisation, presence of necrosis and water content, by generation of DCMs malignant and benign lesions may be differentiated.

Although there are $16^3=4096$ potential colours in the DCMs our technique generates consistent colours for grey and white matter and CSF spaces, however, different tumour types are characterised by specific colour patterns and boundary margins. Preliminary results suggest that our technique is capable of delineating extent of tumour and oedema throughout the entire brain and may represent more accurate boundary definition than conventional imaging. Further validation may allow its application in both diagnosis and delineating extent of tumour for guided surgery or radiotherapy treatment

References: [1] Claus EB, et al., **Cancer** 103:1227-1233, 2005.
[3] Lu S, et al., **AJNR** 24: 937-941, 2003.
[5] Pena A et al., **Br J Radiol** 79:101-109, 2006.

[2] Keles GE et al., **Surg Neurol** 52:371-379, 1999.
[4] Clark CA, et al., **Neuroimage** 20:1601-1608, 2003.

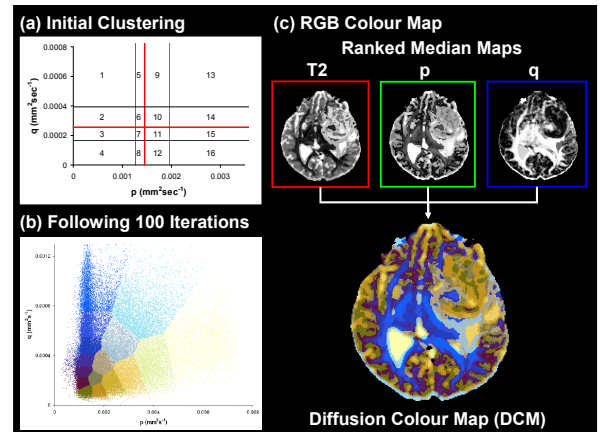


Figure 1: (a) Initial clustering (red lines; medians, black lines; lower & upper quartiles), (b) clusters after 100 iterations. (c) DCM generation.

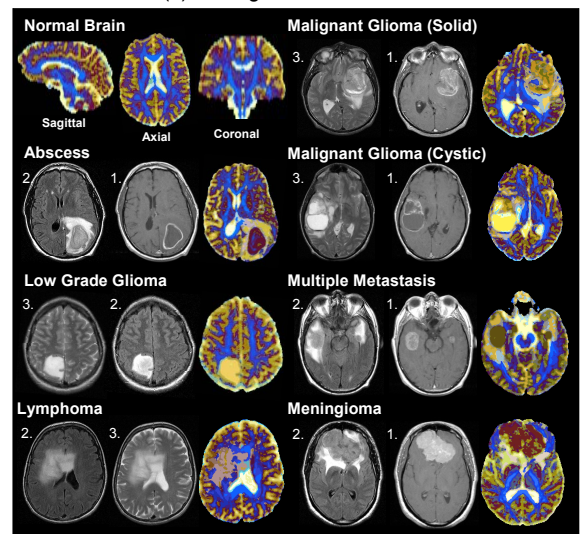


Figure 2: DCM maps created by application to variety of intracranial pathology. (1) T1+Gd, (2) FLAIR, (3) T2.